



IGF26 - 26th International Conference on Fracture and Structural Integrity

Structural optimization of composite steel trussed-concrete beams

M. Deligia^{a,*}, E. Congiu^a, G.C. Marano^b, B. Briseghella^c, L. Fenu^a

^aUniversity of Cagliari, Via Santa Croce 59, Cagliari 09124, Italy

^bPolitecnico di Torino, Corso Duca degli Abruzzi 24, Turin 10129, Italy

^cFuzhou University, No. 2 Xue Yuan Road, University Town, Fuzhou 350108, China

Abstract

The present work deals with the structural optimization of self-supported Composite Steel Trussed-Concrete Beams (CSTCB). CSTCB belongs to the category of prefabricated steel truss embedded in a concrete core casted in situ. The truss is typically composed of a steel plate, which represents the bottom chord, a system of diagonal bars and some coupled rebars working as upper chord. Optimized geometries lead to the minimization of material use. This results in the minimization of the costs, the achievement of sustainability targets, the reduction on the self-weight as well as many architectural advantages. At this purpose, a MATLAB code is herein presented. The code aims to optimize the geometry of the beam by means of a genetic algorithm (*ga*). Two different operative phases, before and after the concrete hardening, which characterize the mechanical response of the beam, are considered within the code. In addition, a case study is developed showing the application of the Matlab code to a homogenized prismatic beam. Advances beyond the state of the art are therefore shown.

© 2021 The Authors. Published by Elsevier B.V.

This is an open access article under the CC BY-NC-ND license (<https://creativecommons.org/licenses/by-nc-nd/4.0>)

Peer-review under responsibility of the scientific committee of the IGF ExCo

Keywords: Steel-Concrete composite beams; Structural optimization; Variable section beams; Optimal design; MATLAB.

Nomenclature

x	longitudinal axis of the beam
h ₀	height of the cross section at the boundaries

h_{0_truss}	height of the truss at the boundaries
b_0	cross section width
L	span
Δh	height reduction at the mid-span
p	pitch of the diagonal bars
s	thickness of the bottom plate
d_{uc}	upper bars diameter
d_{wb}	web bars diameter
c	concrete cover
$J(x)$	variable moment of inertia
J'	first order derivative of the moment of inertia
J''	second order derivative of the moment of inertia
y	vertical displacements
y'	first order derivative of the vertical displacements
y''	second order derivative of the vertical displacements
y'''	third order derivative of the vertical displacements
E	Young modulus of the homogenized beam
γ	material weight of the homogenized beam
q_0	live load

1. Introduction

Composite steel trussed-concrete beams (CSTCBs) consist on a prefabricated steel truss embedded in a concrete matrix casted in situ.



Fig. 1: The self-supported prefabricated steel truss

The first CSTCBs was conceived by the Engineer Salvatore Leone in 1962. The idea was to minimize the production time of a stock of traditional composite beams. He realized that the core and the upper plate of the beams were exuberant. From these considerations, the first CSTCB (Trave REP®) was patented in 1967.

CSTCBs represent a structural typology that lies between the Reinforced Concrete beams and the Composite Steel Concrete ones. The system allows to optimize the performance of the two materials, by simultaneously ensuring a high degree of prefabrication and reducing the instability problems typical of steel members (Mirza & Uy (2009)). Moreover, the steel elements have independent bear capacity and are able to support the own self-weight and the weight of the slabs without any provisional support, as in composite beams occurs. An important aspect that makes standard composite system underperforming is related to the cost of the connections (Lam & El-Lobody (2005)). This problem is overcome in the case of CSTCBs beams, where the connection between the two materials is assigned to the web bars acting as studs, without using other specific connectors. The steel truss represents the reinforcement of

the beam. Although, CSTCBs differ from the traditional RC beams because in the former the static behaviour varies with the construction phase. In particular, two phases are to be considered (Trentadue et al. (2011); Tecnostrutture s.r.l et al. (2011)):

- Phase I - before the hardening of the concrete. Only the steel members are responsible for the mechanical resistance.
- Phase II – after the hardening of the concrete. The concrete core and steel truss contribute together to the mechanical response of the composite beam.

The main practical advantages are that they are partially prefabricated and easily applicable to long spans. This allows to speed the construction schedule, to reduce the cost of labor and, consequently, to lower the general costs. The performance of CSTCB can be advantageously used also in the retrofitting of existing buildings (Sassu et al. (2017)). The design of innovative and performing members and the simplicity of assembly, can have a crucial rule also in the field of static and seismic retrofitting of existing buildings with structural irregularity (Puppio et al. (2019)).

Fig. 2 shows how the prefabrication simplify the management of the site: it is interesting to note that the construction site is free from provisional supports and no formworks are used for the beams because of the presence of the bottom steel plate. This represents an interesting aspect in case of rehabilitation of existing structures, particularly road bridge (Chandrasekaran & Banerjee (2016); Stochino et al. (2018))

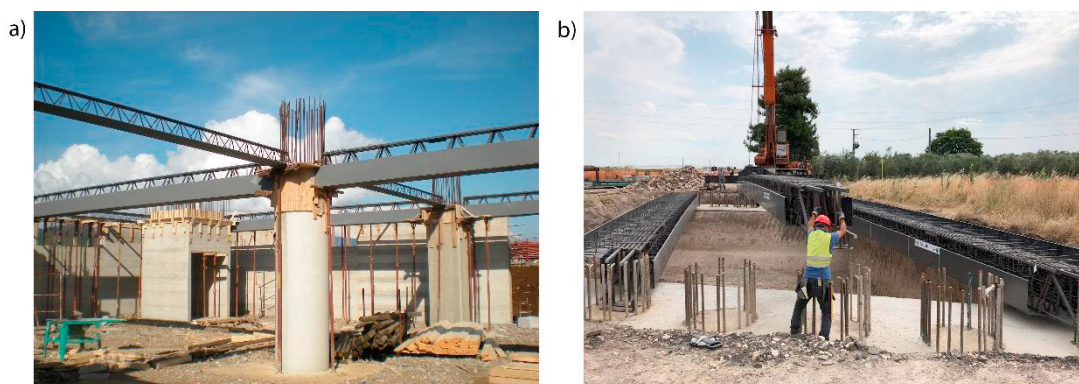


Fig. 2: Pictures from construction sites: a) a residential building; b) a road bridge

1.1. State of the art and scope of the article

CSTCBs are frequently employed in Italy and their behaviour is widely studied in literature through experimental, analytical and numerical investigations. Previous authors have focused their research on several aspects concerning both the first and the second construction phases. In particular, the following issues have been investigated: the flexural and torsional instability of the truss during the first phase (Trentadue et al. (2011); Vincenzi and Savoia (2010)), the welded joint strength (Mendola et al. (2009); Colajanni et al. (2013)), the shear and bending capacity (Chisari and Amadio (2014); Colajanni et al. (2014); Frans and Tahya (2020); Tesser and Scotta (2013); Campione and Colajanni (2016)), the stress transfer mechanism between steel and concrete (Monaco (2014); Colajanni et al. (2014); Colajanni et al. (2015); Tullini and Minghini (2013); Aiello (2008)), the beam to column connection ((Ju et al. (2007); Colajanni et al. (2015); Amadio et al. (2012); Sorgon (2007); Huang et al. (2017)) and the seismic performance (Hsu et al (2004)).

Non-prismatic elements are widely used in several fields, for instance in large span structures. Despite the advantages, like the possibility to optimize the geometry with respect to specific needs, the minimization of material use, the achievement of sustainability targets, the reduction on the self-weight as well as many architectural advantages, solving non-prismatic beams represents a non-trivial problem, and the difficulties in their modelling could lead to inaccurate design and consequently fade the advantages arisen from the optimization. Some authors' research

dealt with the optimal shape of trusses and rectangular section beams (Fiore et al. (2016); Cazacu and Grama (2014); Miguel and Fadel Miguel (2012); Adamu and Karihaloo (1994); Coello and Christiansen (2000); Deb and Gulati (2001); Kaveh and Zolghadr (2014)) and with the solution of variable section beams (De Biagi et al. (2020)). Although, any study has been found in literature concerning neither the shape optimization of CSTCBs nor the design of CSTCBs with variable section. Within this framework, the paper introduces a preliminary study of the structural optimization of CSTCBs.

The manuscript will be organized as follow: paragraph 2 illustrates how the optimization algorithm operates to find the optimal geometry of a CSTCB; within the same section the analytical framework of both the first and the second constructive phases is summarized. Within paragraph 3, an example of the optimization code applied to a homogeneous beam is proposed. The results of the case study are then discussed in paragraph 4.

2. Method

A Matlab code for the optimization of a CSTCB is herein presented. The method consists on a main algorithm, which uses the *ga* solver in Matlab to find the minimum weight of the beam, and on a series of nested function, able to perform the calculation of the beam during the first and the second constructive phases. The flowchart in fig. 3 summarizes the global operation of the code.

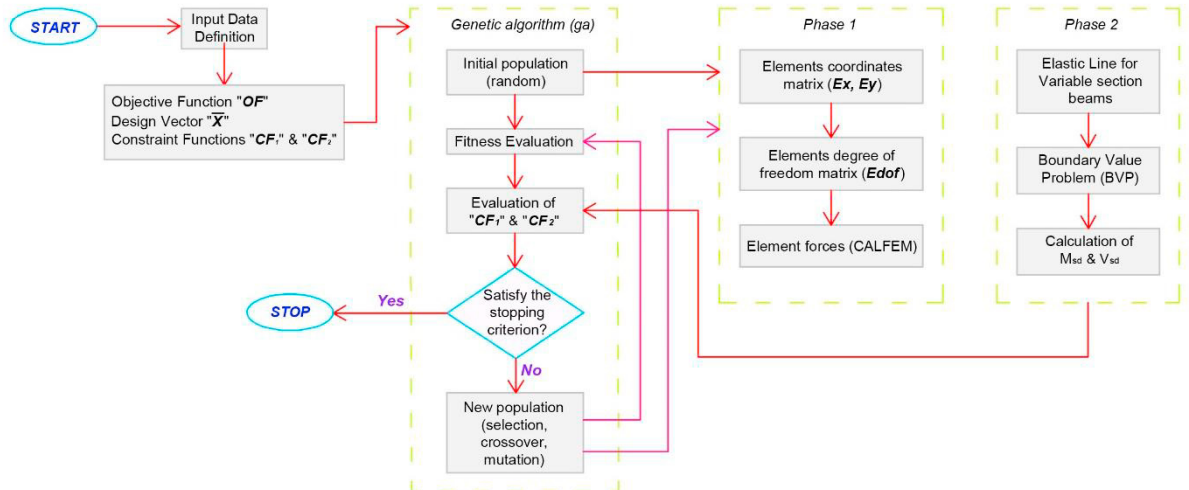


Fig. 3: Algorithm of Optimization for CSTCBs

The algorithm finds the minimum weight of the beam subjected to a series of constraint functions specific for the first and the second constructive phases (CF_I and CF_{II}). It starts with the definition of the input data, characterized by the geometric and mechanical characteristics of the beam and moves to the definition of the objective function (OF), the constraint functions (CF_I and CF_{II}), the design vector (X). A design vector with three design variables is defined. The first design variable is the height reduction at the midspan Δh which determines the shape of the intrados of the beam. The other two design variables are the web diagonals diameter, d_{wb} , and the distance between the diagonals (pitch), p . Fig. 3 shows that by entering the genetic algorithm, a first generation of candidate solutions, expressed in form of design variable vectors, is defined (initial population). Accordingly, the nested functions gradually calculate the mechanical response of the beam during the first and second phase. The OF for that specific population is then evaluated, while the CF s require specific design criteria for phase I and phase II to be satisfied. Over successive generations, thanks to the selection, the crossover and the mutation operations, the population evolves improving the value of the fitness function to be minimized, until an optimal solution is obtained. The algorithm ends when a stopping criterion is reached. Within this code, a maximum number of generations is fixed as stopping criterion.

The main differences between the first and second constructive phases described above concern the following three aspects:

- Cross – section
- Loads conditions
- Boundary conditions

Details on these differences are illustrated within the next paragraphs.

2.1. Phase I: Solution of a simply supported bare truss

During the first phase, only the truss resists against the loads. In particular, the total load results from the sum of the self-weight of the steel truss, the load of the fresh concrete and the load of the slabs. The beam, made exclusively by the steel truss, behaves as a simply supported beam (Fig. 4).

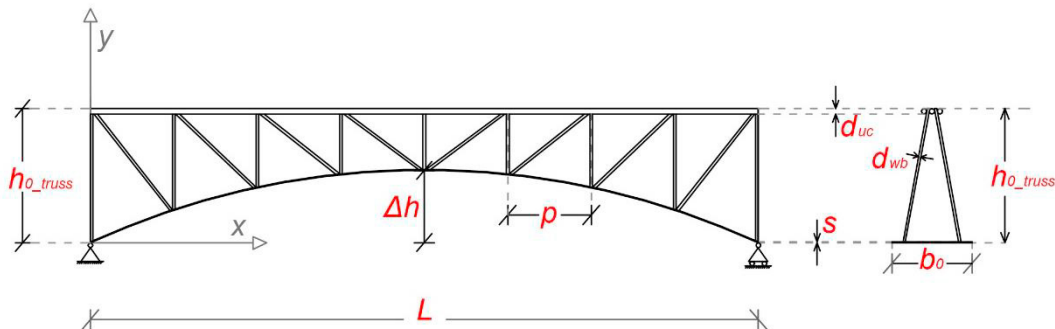


Fig. 4: Static scheme in Phase I

A finite element approach is adopted to solve the steel truss with variable height. At this purpose, the CALFEM (Computer-Aided Learning of the Finite Element Method) is used. It is a Matlab toolbox for finite element applications that increases the versatility and improve the handling of the program. It is based on a series of functions (.m-files), each able to perform a specific operation: calculation of the element stiffness matrix K^e (*bar2e*) and of the global stiffness matrix K (*assem*), computation of the nodal displacements \mathbf{a} (*solve q*). Finally, the elements forces result from the function *bar2s*, concerned specifically for bar elements. Once the beam is solved, the internal forces are verified through the constraint functions defined specifically for the first phase. The CF concern the buckling resistance under bending and compression of the upper and the web bars and the maximum deflection under the loads of the first phase.

2.2. Phase II: Elastic line for beams with variable inertia and Boundary Value Problem

The solution of the second phase is determined by solving the boundary value problem (BVP) deriving from the application of the Elastic-Line formula to the beam with variable height illustrated in Fig. 5.

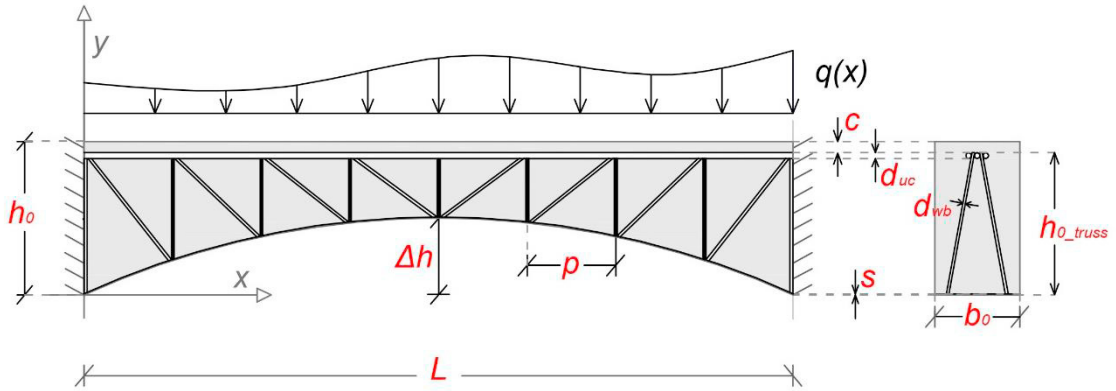


Fig. 5: Static scheme of Phase II

The load $q(x)$ varies along the longitudinal axis x of the beam and the beam is fixed at both ends. The height of the section is expressed as follow:

$$h(x) = h_0 - \Delta h(x) \quad (1)$$

where $\Delta h(x)$ is the emptying function defined by the following equation:

$$\Delta h(x) = \sum_{i=1}^N \Delta h_i \text{sen} \left(i \frac{\pi}{L} x \right) \quad (2)$$

Where i is an odd number and Δh_i is the amplitude. For the sake of simplicity, within this paper $i=1$.

As the BVP is solved, the distribution of the bending moment, $M(x)$, and of the shear forces, $V(x)$, along the beam is calculated by the following equations:

$$M(x) = -EJ(x)y''(x) \quad (3)$$

$$V(x) = -E(J'y'' + Jy''') \quad (4)$$

The internal forces are verified by the constraint functions written specifically for the phase II. In particular, the CF concern the bending resistance, the shear resistance and the maximum deflection at the midspan. The earlier, is calculated according to the Eurocode 4, considering that the steel reinforcement (the truss) is prestressed by the forces and the deformations deriving from the first phase. The shear resistance constraint function results from the multiple truss mechanism.

3. Case study

An example of the optimization code applied to a homogeneous beam is proposed. The shape optimization example is illustrated for the beam shown in fig. 6.

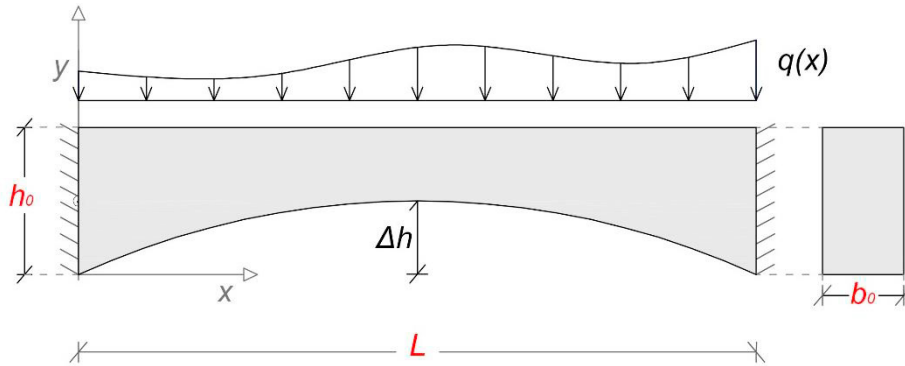


Fig. 6: Case study geometry

The beam has variable height $h(x)$ and constant width b_0 . The section height reduction at the midspan, Δh , is the only optimization parameter considered by this example. The load $q(x)$ varies along longitudinal axis x of the beam, and it results from the sum of two contributes: the dead load, function of the material weight γ and the variable cross section $A(x)$. Unlike the dead load, which is updated for each value of the optimization parameter Δh and varies along the longitudinal axis of the beam, the live load q_0 does not depend on Δh and it is constant along the beam.

The input parameters values are specified in the table:

Table 1. Case study: input parameter

Input parameters			
L	Span	20	m
h_0	Cross-section Height (at the extremities)	2.7	m
b_0	Cross-section width	0.9	m
E	Young Modulus	$36 \cdot 10^6$	kN/m ²
γ	Material weight	25	kN/m ³
q_0	Live Load	90	kN/m

The optimization algorithm finds the minimum volume of the beam subjected to a set of constraint function concerning both the stresses and the vertical displacements:

$$\text{Min } V \quad \text{subjected to} \quad \left\{ \begin{array}{l} \sqrt{\sigma_{max}^2 + 3\tau^2} < \sigma_{id} \\ \sqrt{\sigma^2 + 3\tau_{max}^2} < \sigma_{id} \\ \eta \left(\frac{L}{2} \right) < \frac{L}{250} \end{array} \right. \quad (5)$$

The objective function is the volume of the beam V and it is expressed by the formula:

$$V = b \cdot \int_0^L h(x) dx = b \cdot L \cdot \left(h_0 - \Delta h \frac{2}{\pi} \right) \quad (6)$$

The nested functions in this case study concern only the solution of the BVP and the calculation of the maximum stresses. Thus, once the BVP problem is solved, deformation and stresses are calculated for each population of Δh and the constraint function are evaluated.

$$\sigma_{max} = \frac{6M(x)}{bh^2(x)} \quad (7)$$

$$\tau_{max} = \frac{3V(x)}{2bh(x)} \quad (8)$$

4. Discussion of the results

The following images show the results of the optimization algorithm applied to the homogeneous beam.

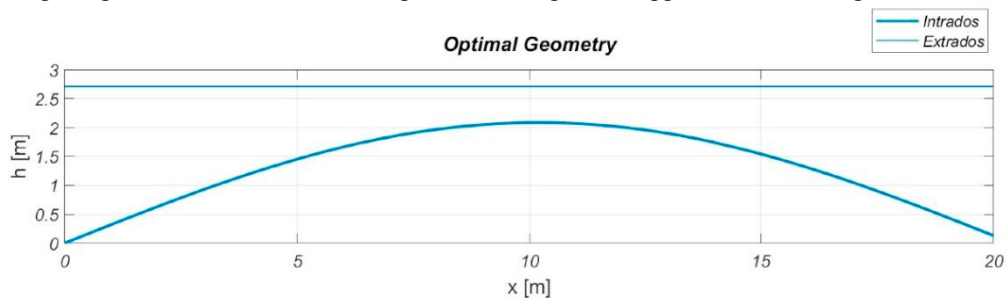


Fig. 7: Optimal Shape of the intrados

Fig. 7 shows the optimal shape of the beam. The volume at the optimal solution is $V_{opt} = 25.37$ m³ against $V_{before} = 49.76$ m³ calculated before the shape optimization. The optimal value of the optimization parameter was $\Delta h_{opt} = 2.09$ m. All the constraint functions were satisfied.

Fig. 8 and Fig. 9 show respectively the distribution of the maximum stresses and of the vertical displacements along the longitudinal axis at the optimal configuration.

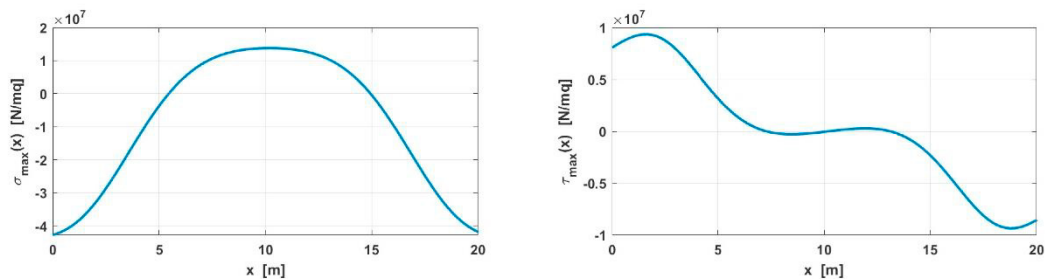


Fig. 8: Distribution of the maximum stresses along the x-axis of the beam.

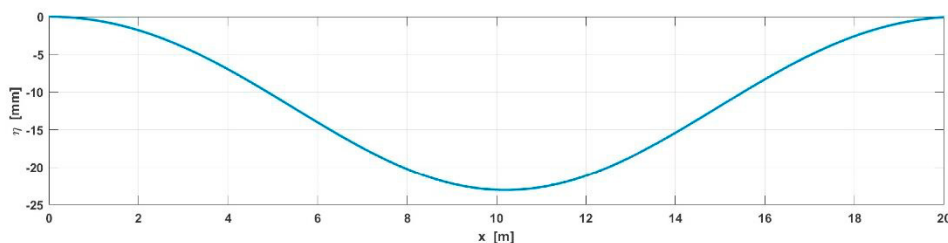


Fig. 9: Vertical displacements [mm]

5. Conclusions

CSTCBs represent very efficient solutions, especially in the case of large span structures. Their behaviour is widely studied in literature by many authors. Although, any previous research dealt neither with the design of CSTCBs with variable section, nor with the shape optimization of this innovative system of beams. Finding the optimal shape of CSTCBs with variable section results in the best possible performance, in the minimization of the materials used and, consequently, in the minimization of the costs. Thus, a preliminary study concerning the shape optimization of CSTCBs with variable height is herein proposed. The distinctive feature of the proposed method is that the algorithm follows the constructive phases of the beam, aiming to optimize simultaneously both the first and the second phase through the fulfilment of specific design criteria.

The method is here applied to a simply supported homogenized beam with a variable cross-section. The results of the case study confirm that the proposed method works properly obtaining a reduction of the volume of about 50%.

The method will be applied to a wide range of design solutions with CSTCBs and further developments are going to be introduced into the proposed code.

References

- Adamu, A. and Karihaloo, B. L. 1994. Minimum cost design of RC beams using DCOE Part I : beams with freely-varying cross-sections. *Structural Optimizaton* 7, 237–251.
- Aiello, M. A. 2008. Analisi sperimentale della connessione acciaio-calcestruzzo nelle travi reticolari miste. *VII Italian Workshop on Composite Structures*, 33–42. <https://iris.unisalento.it/handle/11587/337180?mode=full.27#.YFo9n1VKJIU>
- Amadio, C., Macorini, L., Sorgon, S., Suraci, G., Amadio, C., Macorini, L., Sorgon, S., and Suraci, G. 2012. *A novel hybrid system with RC-encased steel joists*. 8189(2011). <https://doi.org/10.3166/EJECE.15.1433-1463>
- Campione, G. and Colajanni, P. 2016. Analytical evaluation of steel – concrete composite trussed beam shear capacity. *Materials and Structures*, 49(8), 3159–3176. <https://doi.org/10.1617/s11527-015-0711-6>
- Cazacu, R. and Grama, L. 2014. Steel Truss Optimization Using Genetic Algorithms and FEA. *Interdisciplinarity in Engineering (INTER-ENG 2013)*, 12, 339–346. <https://doi.org/10.1016/j.protcy.2013.12.496>
- Chandrasekaran, S. and Banerjee, S. 2016. Retrofit Optimization for Resilience Enhancement of Bridges under Multihazard Scenario. *Journal of Structural Engineering*, 142(8), C4015012. [https://doi.org/10.1061/\(ASCE\)ST.1943-541X.0001396](https://doi.org/10.1061/(ASCE)ST.1943-541X.0001396)
- Chisari, C. and Amadio, C. 2014. An experimental, numerical and analytical study of hybrid RC-encased steel joist beams subjected to shear. *Engineering Structures*, 61, 84–98. <https://doi.org/10.1016/j.engstruct.2013.12.035>
- Coello, C. A. and Christiansen, A. D. 2000. Multiobjective optimization of trusses using genetic algorithms. *Computers and Structures*, 75(6), 647–660. [https://doi.org/10.1016/S0045-7949\(99\)00110-8](https://doi.org/10.1016/S0045-7949(99)00110-8)
- Colajanni, P., La Mendola, L., Latour, M., and Rizzano, G. 2015. FEM analysis of push-out test response of Hybrid Steel Trussed Concrete Beams (HSTCBs). *JCSR*, 111, 88–102. <https://doi.org/10.1016/j.jcsr.2015.04.011>
- Colajanni, P., La Mendola, L., Mancini, G., Recupero, A., and Spinella, N. 2014. Shear capacity in concrete beams reinforced by stirrups with two different inclinations. *Engineering Structures*, 81(1), 444–453. <https://doi.org/10.1016/j.engstruct.2014.10.011>
- Colajanni, P., La Mendola, L., and Monaco, A. 2014. Stress transfer mechanism investigation in hybrid steel trussed – concrete beams by push-out tests. *JCSR*, 95, 56–70. <https://doi.org/10.1016/j.jcsr.2013.11.025>

- Colajanni, P., La Mendola, L., and Monaco, A. 2015. Stiffness and strength of composite truss beam to R.C. column connection in MRFs. *Journal of Constructional Steel Research*, 113, 86–100. <https://doi.org/10.1016/j.jcsr.2015.06.003>
- Colajanni, P., La Mendola, L., and Recupero, A. 2013. Experimental test results vs. analytical prediction of welded joint strength in hybrid steel trussed concrete beams (HSTCBs). *European Journal of Environmental and Civil Engineering*, 17(8), 742–759. <https://doi.org/10.1080/19648189.2013.815135>
- De Biagi, V., Chiaia, B., Marano, G. C., Fiore, A., Greco, R., Sardone, L., Cucuzza, R., Cascella, G. L., Spinelli, M., and Lagaros, N. D. 2020. Series solution of beams with variable cross-section. *Procedia Manufacturing*, 44, 489–496. <https://doi.org/10.1016/j.promfg.2020.02.265>
- Deb, K. and Gulati, S. 2001. Design of truss-structures for minimum weight using genetic algorithms. *Finite Elements in Analysis and Design*, 37(5), 447–465. [https://doi.org/10.1016/S0168-874X\(00\)00057-3](https://doi.org/10.1016/S0168-874X(00)00057-3)
- Fiore, A., Marano, G. C., Greco, R., and Mastromarino, E. 2016. Structural optimization of hollow-section steel trusses by differential evolution algorithm. *International Journal of Steel Structures*, 16(2), 411–423. <https://doi.org/10.1007/s13296-016-6013-1>
- Frans, P. L. and Tahya, H. 2020. *Behavior Of Concrete Beam Deflection Framework System*. 1(1), 151–159. <https://doi.org/10.31098/ic-smart.v1i1.36>
- Hsu, H. Ā., Hsieh, J., and Juang, J. 2004. *Seismic performance of steel-encased composite members with strengthening cross-inclined bars*. 60, 1663–1679. <https://doi.org/10.1016/j.jcsr.2004.04.002>
- Huang, Y., Briseghella, B., Mazzarolo, E., Zordan, T., and Chen, A. 2017. Experimental and numerical investigation of the cyclic behaviour of an innovative prefabricated beam-to-column joint. *Engineering Structures*, 150(January 2018), 373–389. <https://doi.org/10.1016/j.engstruct.2017.07.056>
- Ju, Y. K., Kim, J.-Y., and Kim, S.-D. 2007. Experimental Evaluation of New Concrete Encased Steel Composite Beam to Steel Column Joint. *Journal of Structural Engineering*, 133(4), 519–529. [https://doi.org/10.1061/\(asce\)0733-9445\(2007\)133:4\(519\)](https://doi.org/10.1061/(asce)0733-9445(2007)133:4(519))
- Kaveh, A. and Zolghadr, A. 2014. Democratic PSO for truss layout and size optimization with frequency constraints. *Computers and Structures*, 130, 10–21. <https://doi.org/10.1016/j.compstruc.2013.09.002>
- Lam, D. and El-Lobody, E. 2005. Behavior of Headed Stud Shear Connectors in Composite Beam. *Journal of Structural Engineering*, 131(1), 96–107. [https://doi.org/10.1061/\(asce\)0733-9445\(2005\)131:1\(96\)](https://doi.org/10.1061/(asce)0733-9445(2005)131:1(96))
- Mendola, L. La, Scibilia, N., Agata, V. S., Beams, C. T., Joints, W., Miste, T. R., and Saldati, G. 2009. *Indagine sperimentale su nodi di tralicci in acciaio di travi reticolari miste*. 1(1), 108–125.
- Miguel, L. F. F. and Fadel Miguel, L. F. 2012. Shape and size optimization of truss structures considering dynamic constraints through modern metaheuristic algorithms. *Expert Systems with Applications*, 39(10), 9458–9467. <https://doi.org/10.1016/j.eswa.2012.02.113>
- Mirza, O. and Uy, B. 2009. Behaviour of headed stud shear connectors for composite steel-concrete beams at elevated temperatures. *Journal of Constructional Steel Research*, 65(3), 662–674. <https://doi.org/10.1016/j.jcsr.2008.03.008>
- Monaco, A. 2014. *Experimental analysis, numerical and analytical modeling of shear strength mechanisms in Hybrid Steel Trussed Concrete Beams*. Università degli Studi di Palermo.
- Puppio, M. L., Giresini, L., Doveri, F., and Sassu, M. 2019. Structural irregularity: The analysis of two reinforced concrete (r.c.) buildings. *Engineering Solid Mechanics*, 7(1). <https://doi.org/10.5267/j.esm.2018.12.002>
- Sassu, M., Puppio, M. L., and Mannari, E. 2017. Seismic Reinforcement of a R.C. School Structure with Strength Irregularities throughout External Bracing Walls. *Buildings*, 7(3), 58. <https://doi.org/10.3390/buildings7030058>
- Sorgon, S. 2007. *Analisi di un sistema ibrido sismo – resistente costituito da elementi tralicciati in acciaio inglobati nel calcestruzzo*. Università degli studi di Trieste.
- Stochino, F., Fadda, M. L., and Mistretta, F. 2018. Low cost condition assessment method for existing RC bridges. *Engineering Failure Analysis*, 86(December), 56–71. <https://doi.org/10.1016/j.engfailanal.2017.12.021>
- Tecnostrutture s.r.l. Comitato scientifico REP®: prof. ing. Braga, F., prof. ing. Calvi, G. M., prof. ing. Landolfo, R., ing. Scotta, R., and prof. ing. arch. Siviero, E. 2011. *Progettare con il sistema REP®: Travi REP®, Pilastri e Setti - Strutture miste autoportanti acciaio e calcestruzzo secondo normativa vigente*.
- Tesser, L. and Scotta, R. 2013. Flexural and shear capacity of composite steel truss and concrete beams with inferior precast concrete base. *Engineering Structures*, 49, 135–145. <https://doi.org/10.1016/j.engstruct.2012.11.004>
- Trentadue, F., Marano, G. C., Quaranta, G., and Mastromarino, E. 2011. *La instabilità delle travi reticolari miste autoportanti* (WAVENG s.r.l (ed.)).
- Tullini, N. and Minghini, F. 2013. Nonlinear analysis of composite beams with concrete-encased steel truss. *Journal of Constructional Steel Research*, 91, 1–13. <https://doi.org/10.1016/j.jcsr.2013.08.011>
- Vincenzi, L. and Savoia, M. 2010. Stabilità di tralicci PREM in prima fase. *Proceedings of the 18th C.T.E. Congress*, 849–858.